The EMBO Journal (2006) 25, 2723–2734 | © 2006 European Molecular Biology Organization | All Rights Reserved 0261-4189/06
www.embojournal.org

THE EMBO JOURNAL

Myc influences global chromatin structure

Paul S Knoepfler[1], Xiao-yong Zhang[2], Pei Feng Cheng[1], Philip R Gafken[3], Steven B McMahon[2] and Robert N Eisenman[1,*]

[1]Division of Basic Sciences, Fred Hutchinson Cancer Research Center, Seattle, WA, USA, [2]The Wistar Institute, Gene Expression and Regulation Program, Philadelphia, PA, USA and [3]Proteomics Facility, Fred Hutchinson Cancer Research Center, Seattle, WA, USA

The family of *myc* proto-oncogenes encodes transcription factors (c-, N-, and L-Myc) that regulate cell growth and proliferation and are involved in the etiology of diverse cancers. Myc proteins are thought to function by binding and regulating specific target genes. Here we report that Myc proteins are required for the widespread maintenance of active chromatin. Disruption of N-*myc* in neuronal progenitors and other cell types leads to nuclear condensation accompanied by large-scale changes in histone modifications associated with chromatin inactivation, including hypoacetylation and altered methylation. These effects are largely reversed by exogenous Myc as well as by differentiation and are mimicked by the Myc antagonist Mad1. The first chromatin changes are evident within 6 h of Myc loss and lead to changes in chromatin structure. Myc widely influences chromatin in part through upregulation of the histone acetyltransferase GCN5. This study provides the first evidence for regulation of global chromatin structure by an oncoprotein and may explain the broad effects of Myc on cell behavior and tumorigenesis.

The EMBO Journal (2006) **25,** 2723–2734. doi:10.1038/sj.emboj.7601152; Published online 25 May 2006
Subject Categories: chromatin & transcription; development
Keywords: chromatin; epigenetics; histone modification; Myc; stem and progenitor cells

Introduction

The members of the Myc/Mad/Mnt superfamily of basic helix–loop–helix zipper (bHLHZ) transcription factors each heterodimerize with the bHLHZ protein Max and bind the E-box sequence CACGTG. Transcriptional activation by Myc proteins and repression by Mad/Mnt proteins, at E-box binding sites, are involved in regulation of cell growth, proliferation, and apoptosis (Eisenman, 2001). Targeted disruption of c-*myc*, N-*myc*, or *max* in the mouse leads to embryonic lethality (Stanton *et al*, 1992; Davis *et al*, 1993; Shen-Li *et al*, 2000), whereas overexpression of *myc* genes is strongly associated with the genesis of diverse cancers in many species (Lutz *et al*, 2002). Myc activates transcription through recruitment of chromatin-modifying complexes. For example, interaction with the coactivator TRRAP mediates Myc's association with histone acetyltransferases (HATs) GCN5 and Tip60 (McMahon *et al*, 1998, 2000; Frank *et al*, 2003). Myc also interacts with CBP and the chromatin-remodeling complex containing Ini1 (Cheng *et al*, 1999; Vervoorts *et al*, 2003). By contrast, Mad proteins recruit histone deacetylases (HDACs) via the corepressor mSin3 (Ayer, 1999; Knoepfler and Eisenman, 1999). The complexes recruited by Myc–Max and Mad–Max induce distinct chromatin modifications within the regulatory regions of shared target genes, leading to activation or repression (Eisenman, 2001; Frank *et al*, 2001; Fernandez *et al*, 2003). The notion that Myc is a typical transcription factor regulating the expression of a small number of target genes has been challenged by recent findings indicating that DNA binding and gene regulation by Myc are both surprisingly widespread (Fernandez *et al*, 2003; Li *et al*, 2003; Orian *et al*, 2003; Cawley *et al*, 2004; Patel *et al*, 2004). To study potential global gene regulatory functions of Myc, we focused on *myc* loss-of-function mutations in cells and tissues normally dependent on Myc activity.

*Corresponding author. Division of Basic Sciences, Fred Hutchinson Cancer Research Center, 1100 Fairview Avenue N, Seattle, WA 98109-4417, USA. Tel.: +1 206 667 4445; Fax: +1 206 667 6522;
E-mail: eisenman@fhcrc.org

Received: 6 December 2005; accepted: 27 April 2006; published online: 25 May 2006

Results

Altered nuclei and histone modifications in N-myc null cells

We previously demonstrated that N-*myc* is essential for normal nervous system development (Knoepfler *et al*, 2002) by using nestin-cre to generate a nervous system-specific conditional knockout of N-*myc* in the mouse (N-*myc* NS null). In N-*myc* NS null E12.5 embryos, we observed that neural stem and progenitor cell (NPC) nuclei were abnormally small, round, and dark when stained with either H&E or methyl green (compare control and N-*myc* null nuclei in Figure 1Ai–ii and Supplementary Figure S1A). Both TUNEL and caspase cleavage assays demonstrated that these changes are not due to increased apoptosis in the N-*myc* null tissues and cells (Knoepfler *et al*, 2002) (Supplementary Figure S2A and B), and assays for senescence-associated β-gal activity indicated that they are not due to senescence (Supplementary Figure S2C). We therefore examined whether the changes in nuclear morphology might reflect alterations in chromatin.

Transcriptional activity of chromatin is associated with specific histone modifications, including acetylation and methylation (Strahl and Allis, 2000), implicated in local gene-specific effects as well as global chromatin structure (Vogelauer *et al*, 2000; Rea *et al*, 2000; Berger and Felsenfeld, 2001; Kurdistani *et al*, 2004; Schubeler *et al*, 2004). To determine if disruption of Myc function induces changes in histone modifications consistent with chromatin inactivation, we first employed immunohistochemistry (IHC) to assess global levels of acetylated histone H3 and H4 (AcH3, AcH4) in the developing nervous system of control, N-*myc* NS null (Knoepfler *et al*, 2002), and nestin-N-*myc* transgenic (Tg) E12.5 embryos (Figure 1Av–viii). In these IHC studies, anti-AcH3 staining is K9 specific, whereas anti-AcH4 staining recognizes H4 acetylated at K5, K8, K12, and K16.

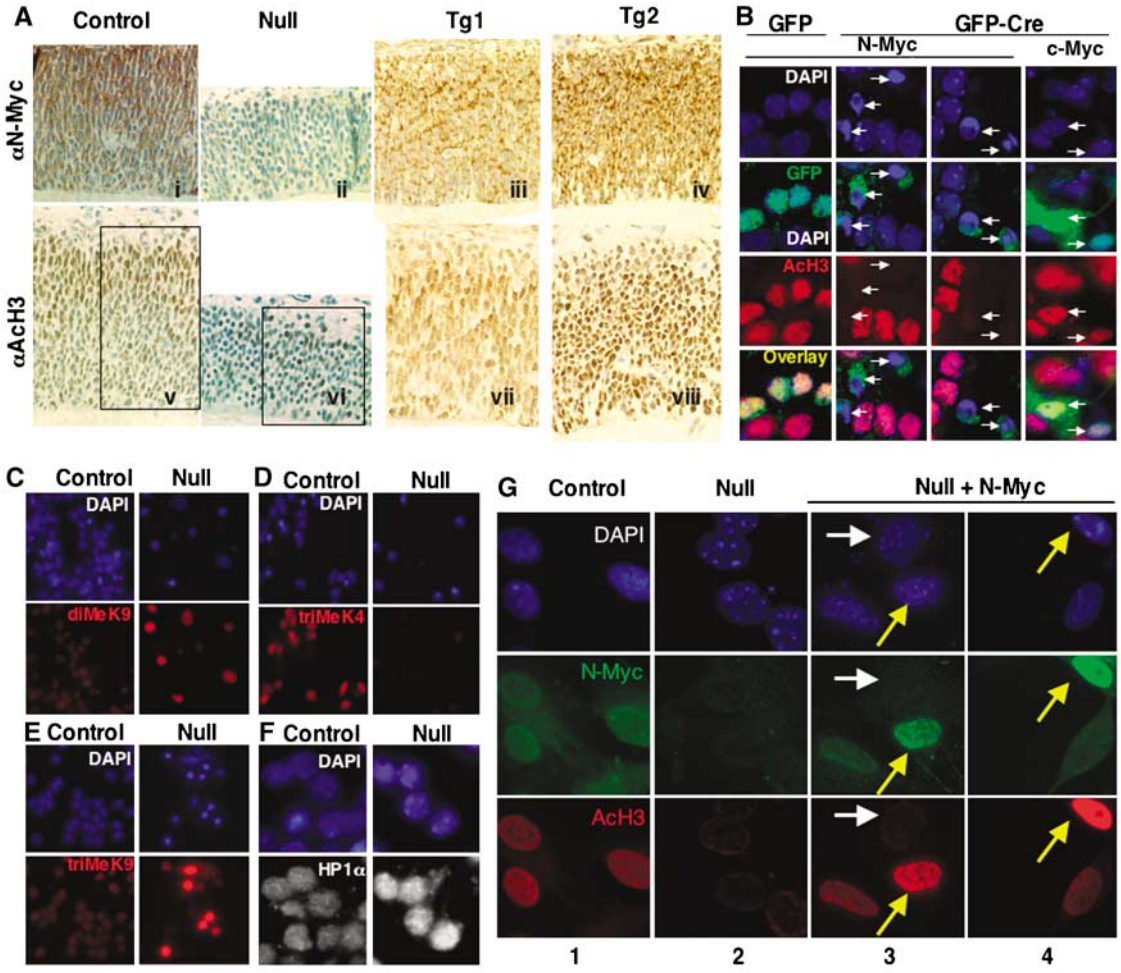

Figure 1 Analysis of N-Myc levels and histone acetylation. (**A**) E12.5 Sagittal sections from control (panels i and v), N-*myc* null (panels ii and vi), and N-*myc* transgenic embryos (Tg) expressing moderately (iii and vii) and highly elevated levels of N-Myc (iv and viii) under control of the nestin promoter/enhancer. Embryos were stained for N-Myc (brown stain, panels i–iv) and AcH3 (brown stain; panels v–viii) and counterstained with methyl green (bluish). Nuclear and cytoplasmic N-Myc proteins are evident, as has been previously reported (Wakamatsu *et al*, 1993) (× 100 magnification). Boxed regions are shown at higher magnification in Supplementary Figure S1A. (**B**) CGNPs derived from N-*myc*$^{flox/flox}$ (left three columns) or c-*myc*$^{flox/flox}$ (right column) embryos were grown in medium containing Shh (3 ng/ml), infected with GFP or Cre-IRES-GFP retroviruses, and stained with DAPI and anti-AcH3. White arrows denote infected cells. (**C–F**) Control and nestin-cre-derived N-*myc* null CGNPs stained for DAPI (blue) and histone H3 diMeK9 (**C**), triMeK4 (**D**), and triMeK9 (**E**) (red). (**F**) Control and N-*myc* null CGNPs stained for DAPI (blue) and HP1α (monochrome). (**G**) Cultured E12.5-derived control and N-*myc* null neurospheres stained for DNA (DAPI), N-Myc (green), and AcH3 (red). Columns 3 and 4 represent null cells transfected with N-Myc. White arrow indicates untransfected cell. Yellow arrows indicate NPCs with supraphysiological levels of N-Myc. Control (flox/flox) and null (flox/flox nestin-cre) cultures were grown for at least 1 month before these analyses and exhibited a high degree of stability in culture composition and properties (extremely low, but similar rates of spontaneous differentiation, stable proliferation rates, stable neurosphere morphology and size, and stable cellular morphology upon growth as a monolayer). We consistently observed that 80–90% of the N-*myc*$^{flox/flox}$ nestin-cre + neurosphere cells exhibited a complete loss of detectable N-Myc protein.

Acetylation of each of these lysines is associated with active chromatin (Turner *et al*, 1992; Jeppesen and Turner, 1993; Braunstein *et al*, 1996). In the ventricular zone (VZ) of control embryos, we noted a positive correlation between nuclear size and the levels of N-Myc, AcH3, and AcH4 (Figure 1Ai and v and Supplementary Figure S1A and C). N-*myc* null NPCs exhibited striking histone hypoacetylation (low/absent brown stain) specifically associated with abnormally small round nuclei that also counterstained darkly with the DNA dye methyl green, suggesting chromatin condensation (Figure 1Ai–ii and v–vi).

We next asked whether acute disruption of N-*myc* would also alter histone acetylation. Using cultured N-*myc*$^{flox/flox}$ cerebellar granule neural progenitors (CGNPs), N-*myc* was acutely disrupted by infection with MSCV Cre-IRES-GFP (Cre-GFP), a retroviral vector expressing Cre and GFP (Figure 1B). Disruption of N-*myc* in a majority of GFP$^+$ cells was verified by immunofluorescence staining (IF) for endogenous nuclear N-Myc protein (not shown), similar to the large fraction of cells with N-*myc* loss in CGNPs with nestin-cre-driven knockout (Supplementary Figure S3A). N-Myc-deficient GFP + CGNPs exhibit dramatic changes in histone acetylation, with the majority having an apparently complete loss of detectable histone H3 and H4 acetylation (Figure 1B, white arrows in column 3; data not shown). These changes are associated with nuclear condensation and alterations in DAPI staining (see below). Importantly, Cre-GFP virus had no effect on histone acetylation in c-*myc*$^{flox/flox}$ (de Alboran

et al, 2001) CGNPs, consistent with the report that c-*myc* is not expressed in CGNPs (Kenney *et al*, 2003) (Figure 1B). Further, infection of N-*myc*$^{flox/flox}$ CGNPs with MSCV IRES-GFP virus, which only expresses GFP, had no effect on acetylation or nuclear structure (Figure 1B, column 1). Disruption of N-*myc* also does not appear to influence CGNP identity or culture composition. Control and null CGNP cultures exhibit essentially identical fractions (84–87%) of cells staining with the CGNP-specific marker Zic1 (Aruga *et al*, 1994) (Supplementary Figure S3B). Our data indicate that loss of Myc from neuronal progenitors is associated with significantly decreased levels of H3 and H4 acetylation.

Myc is required for maintenance of normal histone methylation patterns

To determine whether the decreased histone acetylation observed in N-*myc* null cells correlates with altered histone methylation patterns (Rea *et al*, 2000), we began by staining CGNPs for methylated H3-K9. Control (N-*myc*$^{flox/flox}$) CGNPs displayed only faint speckled staining for both H3-diMeK9 (Figure 3A, top panel of column 8, and Figure 1C) and H3-triMeK9 (Figure 1E), marks of repressive chromatin. In contrast, we found that N-*myc* null (N-*myc*$^{flox/flox}$ nestin-cre) CGNPs exhibited high levels of H3-diMeK9 and H3-triMeK9 (Figures 1C, E, and 3A, column 8). Moreover, N-*myc* null CGNPs show a dramatic reduction in H3-triMeK4, a modification strongly associated with active chromatin (Strahl and Allis, 2000) (Figure 1D). We see the same general pattern of histone methylation changes in Tet-Off Myc B cells (Supplementary Figure S4) and, to a lesser extent, in c-*myc* null fibroblasts (not shown). The heterochromatin binding protein HP1α, which has been shown to directly interact with H3-MeK9 (Bannister *et al*, 2001; Lachner *et al*, 2001), exhibits a focal nuclear staining pattern evident in control CGNPs (Figure 1F) similar to that reported in other studies (Lachner *et al*, 2001). Consistent with their high levels of H3-di-MeK9 and H3-tri-MeK9, N-*myc* null CGNPs exhibit unusually intense and abundant HP1α foci (Figure 1F), presumably reflecting abnormal spreading of heterochromatin (see below). In summary, our targeted deletion experiments indicate that an apparently general loss of histone acetylation, increased histone methylation, and chromatin condensation in the N-*myc* null CGNPs are associated with loss of N-*myc*.

Reintroduction of Myc restores altered histone acetylation in N-myc null cells

To ascertain if the decreased levels of histone acetylation represent an irreversible cellular response to N-Myc loss, we examined N-*myc* null (N-*myc*$^{flox/flox}$ nestin-cre+) neurosphere cultures derived from E12.5 whole embryonic brains. Overall IF analysis indicated that such N-*myc* null neurosphere cultures exhibited very low or undetectable nuclear histone acetylation compared to N-myc$^{flox/flox}$ controls (Figure 1G, columns 1 and 2). Introduction of N-Myc (Figure 1G, columns 3 and 4, and Figure 5G) or c-Myc (data not shown) into null cells resulted in markedly increased acetylation within 2 days of transfection. In the subset of N-*myc* null neurospheres, which expressed supraphysiological levels of introduced N-Myc, histone acetylation increased to substantially above normal (Figure 1G, yellow arrows). In addition, VZ cells in N-*myc* Tg mice displayed above-normal H3 and H4 acetylation (Figure 1Aiii, iv, vii, and viii and Supplementary Figure S1B) consistent with the notion that Myc levels are linked to the extent of histone acetylation. Such N-*myc* overexpression and hyperacetylation is also associated with VZ hyperplasia (Supplementary Figure S1B). Restoration of histone acetylation is strongly attenuated in N-*myc* null neurospheres transfected with N-*myc* mutants lacking Myc Box II (MBII), a highly conserved transactivation domain that associates with the HAT-binding coactivator TRRAP (McMahon *et al*, 2000), or lacking the C-terminal basic region, which is required for DNA binding (Supplementary Figure S10). We note that overexpression of the transcription factor E2F had no apparent effect on widespread histone acetylation (Supplementary Figure S9).

Quantitative analysis of chromatin changes

Because quantitative analyses require more chromatin than can be readily obtained from our primary murine neuronal cell cultures, we turned to the well-characterized c-*myc* null rat fibroblast cell line, HO15.19 (Mateyak *et al*, 1997). As in the neuronal cells, HO15.19 cells lacking c-*myc* (hereafter 'c-*myc* null' and which do not express N- or L-*myc*) (Mateyak *et al*, 1997) are hypoacetylated at H3 and H4 compared to the TGR wild-type (WT) parental control line when assayed by IF (Figure 2A; data not shown). Reintroduction of c-Myc into the c-*myc* null cells increases histone acetylation levels to WT (Figure 2A). In three independent immunoblotting experiments, loss of c-*myc* resulted in approximately two-fold reductions in AcH3 and AcH4 compared to total histone levels, whereas there were no consistent changes in total histone levels associated with *myc* status. These reductions are largely reversed following reintroduction of c-*myc* (Figure 2C). Loss of detectable c-Myc protein in the c-*myc* nulls and its restoration in the cells with reintroduced c-Myc have been previously verified (Mateyak *et al*, 1997; Shiio *et al*, 2002).

Histone modification changes associated with loss of *myc* were also studied by mass spectrometric (MS) analysis of acid extracts from parental control TGR cells and *c-myc* null fibroblasts (Figure 2D and E). MS analysis of cumulative H4 acetylation at K5, 8, 12, and 16 was consistent with widespread histone hypoacetylation in the c-*myc* null cells (Figure 2D and E). The level of completely unmodified H4 peptide was approximately 20% higher in nulls, which also exhibited a nearly 20% reduction in monoacetylation. Histone H4 isolated from nulls had approximately two-fold reductions in di, tri-, and tetra-acetylation. Thus, the overall degree of decreased H4 acetylation in nulls determined by MS and immunoblotting is comparable (Figure 2C). We next examined site-specific acetylation in controls and nulls and found decreased acetylation of all four lysine residues in the nulls (Figure 2E). The site-specific and total lysine acetylation MS data taken together suggest that the histone H4 hypoacetylation that results from loss of Myc is primarily due to a loss of 1–2 acetyl groups, predominantly from K12 and K16, from poly-acetylated histone H4 leading to a shift toward mono- and unacetylated H4 amino-termini.

Myc influences global histone modification, nuclear size, and heterochromatin

We consistently observe a correlation between levels of N-Myc, nuclear size, and acetylated H3 and H4 in neural progenitors. Figure 3A shows conditional knockout (N-*myc*$^{FL/FL}$ nestin-cre) CGNPs arranged in the order of

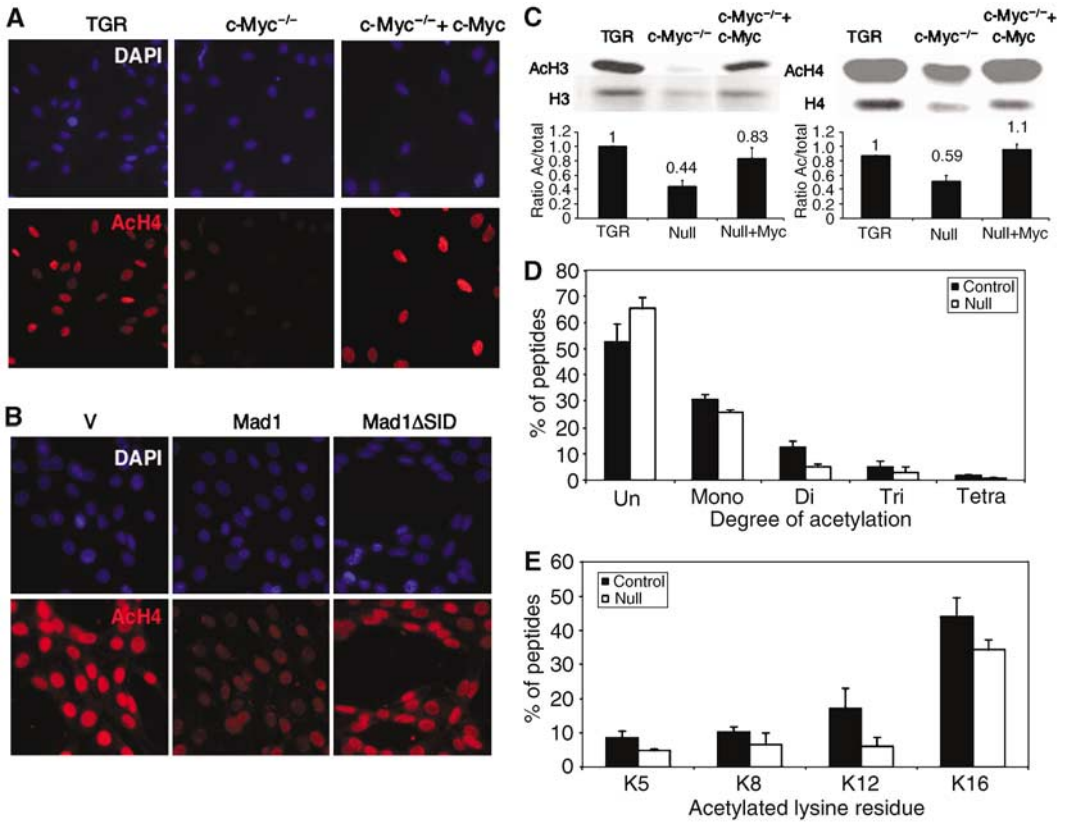

Figure 2 Histone modifications in c-*myc* null, *mad1*–transfected, and WT fibroblasts. (**A**) Staining for AcH4 (red) in parental (TGR), c-*myc* null (HO15.19), and c-*myc* null rat fibroblasts stably transfected with c-*myc*. (**B**) Mad1 overexpression in WT murine fibroblasts partially phenocopies loss of Myc. (**C**) Immunoblotting for the indicated acetylated and methylated histones H3 and H4 comparing levels in TGR, c-*myc* null, and c-*myc* null rat fibroblasts transfected with c-*myc*. Values in the graphs represent the ratio of arbitrary values measured by Odyssey system for bands representing modified/total histones from three independent biological repeats. (**D, E**) Mass spectrometric data on total and K-specific histone H4 N-terminal acetylation from three independent experiments. The relative fraction of N-terminal peptides containing 0–4 acetyl groups was determined as well as the fraction of specific K residues that were acetylated. All error bars in this figure are s.e.m.

decreasing nuclear size. Varying levels of residual N-Myc protein remain in a small subset of these conditionally null CGNPs and N-Myc level correlates with nuclear size and histone acetylation (Figure 3A, columns 1–6; data not shown). These findings suggest that loss of histone acetylation parallels decreasing levels of Myc (column 6). This notion is also supported by the observation that in cultures of conditionally null CGNPs, the small subset with residual N-Myc levels are the only ones with remaining detectable, albeit low, levels of histone acetylation (Supplementary Figure S3A). Interestingly, the subnuclear localization pattern of N-Myc broadly overlaps with regions of anti-AcH3 and anti-AcH4 IF, all of which are excluded from islands of intense DAPI staining (Figure 3A, column 6), characteristic of heterochromatin (Bickmore and Craig, 1997). Also evident is a correlation between H3-diMeK9 levels, decreased nuclear size, and the extent of heterochromatic regions (Figure 3A, columns 7 and 8). A more detailed analysis of nuclear and DNA structure in control and N-*myc* null CGNPs was conducted using transmission electron microscopy (EM) of uranyl acetate-stained cells. As shown in Figure 3B, nuclei from control CGNPs are approximately 5–10 μm in diameter composed predominantly of lightly stained euchromatic regions, with the exception of 3–5 darkly staining heterochromatic regions (Busch, 1974) (arrows in Figure 3Bi). These darkly staining regions, each approximately 0.5–1 μm across, are frequently associated with the nuclear lamina, as expected for heterochromatin (Cohen *et al*, 2001). They are similar in size, location, and appearance to the intense DAPI foci in CGNPs (Figure 3B, white arrows in panel ii), which have been established to be heterochromatin in murine cells (Bickmore and Craig, 1997). In N-*myc* null CGNPs, the majority of nuclei are several fold smaller in area compared to controls and the heterochromatic regions are greatly expanded (Figure 3Biii–v). Thus, loss of Myc results in a decrease in nuclear volume and a striking spreading of heterochromatin, no longer limited to foci, throughout the nuclei of null cells.

Loss of Myc leads to decreased DNA accessibility

To address whether *myc* levels influence chromatin structure, we conducted micrococcal nuclease (MNase) accessibility assays (Weintraub and Groudine, 1976) using the well-established Tet-Off Myc B (P493-6) cell system (Schuhmacher *et al*, 1999) in which Myc can be reproducibly turned off by the addition of tetracycline. The P493-6 cells exhibit the same type of chromatin changes upon Myc downregulation as observed in *myc*-deficient neuronal cells and fibroblasts (see below). Intact living cells were permeabilized so as to minimize effects on chromatin structure (Zaret, 1999) and cells were treated with increasing amounts of MNase (Figure 3C). In the absence of MNase, neither Myc-Off nor

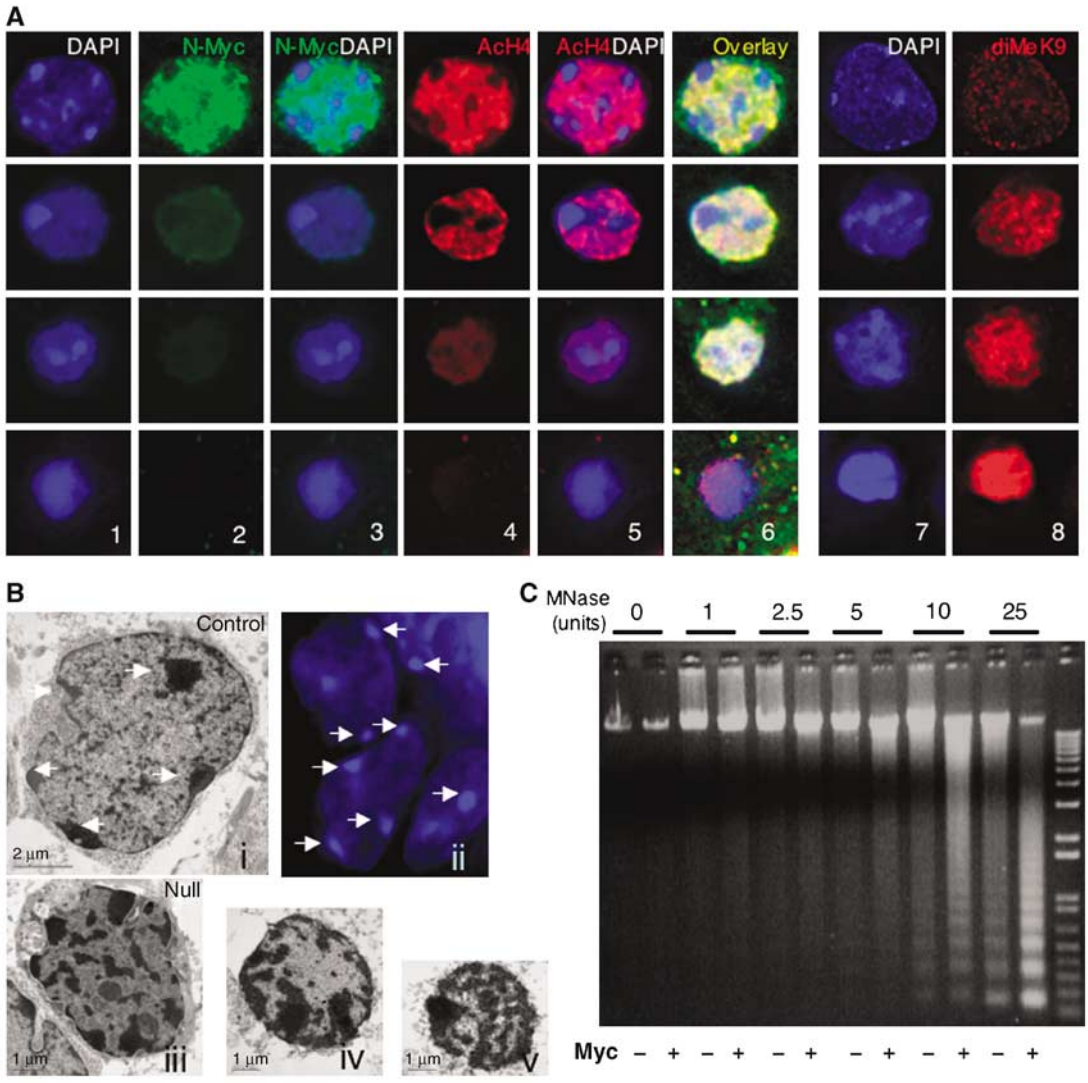

Figure 3 Histone modifications, heterochromatin, and DNA accessibility in control and null N-*myc* CGNPs. (**A**) N-*myc*$^{flox/flox}$ nestin-cre CGNPs were visually sorted by nuclear size following staining with the indicated antibodies. Each color intensity in column 6 was uniformly increased in each panel to maximize detection of potential colocalization of signal. (**B**) Control (top) and N-*myc* null (bottom) CGNPs were analyzed by EM following uranyl acetate staining (panels i and iii–vi) or by DAPI (panel ii). Arrows indicate heterochromatic regions. Note: Although the scale bar in panel (i) is 2 μm and the bars in the other panels are 1 μm, the bar in (i) is also twice as long as the bars in the other panels, indicating that all images are exactly of the same magnification. (**C**) MNase assay on Tet-off Myc B cells with and without 72 h of tetracycline treatment.

Myc-On cells exhibited evidence of endogenous nuclease activity. However, at increasing concentrations of MNase, Myc-Off cells exhibited a strongly enhanced resistance to MNase, indicative of a more closed chromatin structural state (Shogren-Knaak *et al*, 2006). We have observed decreased accessibility following Myc loss in four independent experiments in these cells. Thus, Myc appears to influence DNA accessibility, consistent with the histone modifications described above. These data support the notion that Myc has a widespread influence on chromatin structure.

Loss of Myc rapidly alters histone modifications in a cell cycle- and differentiation-independent manner

To assess the kinetics of chromatin changes associated with loss of Myc, we analyzed Tet-Off Myc B cells (Schuhmacher *et al*, 1999) in which introduction of tetracycline shuts down c-Myc expression. Expression of endogenous Myc proteins is undetectable in these cells, and introduction of tetracycline rapidly (within 16 h) leads to strong downregulation of the c-Myc transgene (Grandori *et al*, 2003). Introduction of tetracycline for 72 h in a serum-free context resulted in loss of Myc (data not shown) as well as the same general pattern of changes we observed in neuronal cells and fibroblasts upon Myc disruption: decreased histone H3 K9 acetylation and K4 methylation as well as increased levels of H3-diMeK9, and nuclear condensation (Supplementary Figure S4; not shown). Initial changes were detectable as early as 6 h after introduction of tetracycline (Supplementary Figure S4) and downregulation of Myc (data not shown), whereas more substantial changes were evident after 24 and 72 h. Thus, changes in histone modifications occur rapidly following alterations in Myc levels. Further, the changes in chromatin do not appear to be secondary to changes in cell cycle status because the chromatin alterations are observed with loss of

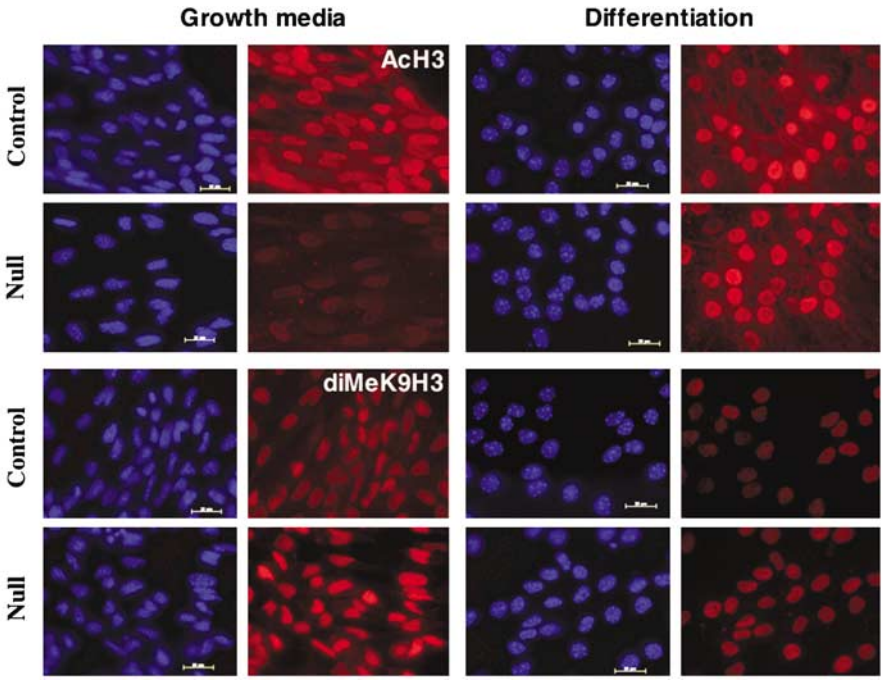

Figure 4 Differentiation of control and N-*myc* null neurospheres influences histone modifications. IF staining of control and N-*myc* null neurospheres induced to differentiate for 7 days by growth factor withdrawal and retinoic acid treatment.

Myc in a system in which there are no cycling cells (serum-free conditions) (Schuhmacher *et al*, 1999).

Several additional lines of evidence argue against the possibility that the changes in histone modifications are secondary consequences of cell cycle arrest upon Myc loss. The *c-myc* null HO15.19 fibroblasts, which exhibit decreased acetylation (Figure 2), proliferate, albeit at a lower rate (Mateyak *et al*, 1997). Similarly, nestin-cre-derived N-*myc* null and WT CGNPs express Ki67 (Supplementary Figure S5C), a nuclear antigen present in cycling but not quiescent cells (Gerdes *et al*, 1991). Furthermore, we found that a subset of N-*myc* null CGNPs, even those with the most extreme nuclear condensation and histone hypoacetylation, nonetheless exhibited anti-BrdU and anti-phosphoH3 staining (Supplementary Figure S5A and B; data not shown). We have also observed that differentiation of neurospheres and CGNPs, associated with terminal cell cycle arrest, leads to increased histone acetylation and decreased H3-K9 methylation (Figure 4; not shown). Furthermore, a recent study indicates that quiescent lymphocytes exhibit a striking decrease in repressive histone methylation marks compared to activated, proliferating cells (Baxter *et al*, 2004). Taken together, these data argue that the changes observed upon Myc loss of function are not simply a consequence of proliferation arrest.

The Myc antagonist Mad1 suppresses widespread histone acetylation: a role for the global balance of HDACs and HATs

Mad-related proteins exhibit widespread genomic binding in *Drosophila* overlapping with dMyc binding sites (Orian *et al*, 2003) and antagonize some Myc functions through shared target genes in mammalian cells (Iritani *et al*, 2002). We asked whether Mad1 also influences widespread chromatin modification. Mad1 overexpression in control neurospheres (not shown) and murine fibroblasts resulted in a pronounced reduction in global AcH4 (Figure 2B) and AcH3 (not shown) levels in both cell types. Furthermore, deletion of the Mad1 SID domain (Mad1ΔSID), which constitutes the binding site for the mSin3–HDAC corepressor complex, largely abrogated Mad1-induced suppression of histone acetylation (Figure 2B). In contrast to Mad1, overexpression of Max had no discernable effects on global chromatin in either fibroblasts or in WT neurospheres and Max was also unable to reverse the histone hypoacetylation in *myc* null neurospheres (data not shown). These findings were expected given that Max is required for the opposing activities of Myc as well as Mad proteins (Eisenman, 2001).

We hypothesized that the widespread alterations in chromatin owing to changes in Mad or Myc could be due to a large-scale imbalance in the overall levels of HATs and HDACs. The HDAC inhibitor TSA reversed histone hypoacetylation in N-*myc* null neurospheres (Supplementary Figure S6A), suggesting that loss of Myc may cause chromatin changes in part by shifting the balance of HDACs and HATs toward HDACs. This notion is also supported by our observation that overexpression of HDAC1 in fibroblasts phenocopies loss of Myc (Supplementary Figure S6B) in terms of nuclear condensation as well as histone hypoacetylation. Furthermore, introduction of the HATs GCN5, MOF, or TIP60 reverses the histone hypoacetylation observed in N-*myc* null neurospheres (Figure 5G; not shown).

GCN5 is a direct Myc target gene

One mechanism by which Myc could control the overall equilibrium of histone-modifying enzymes is by regulation of their expression. In order to address this possibility, levels

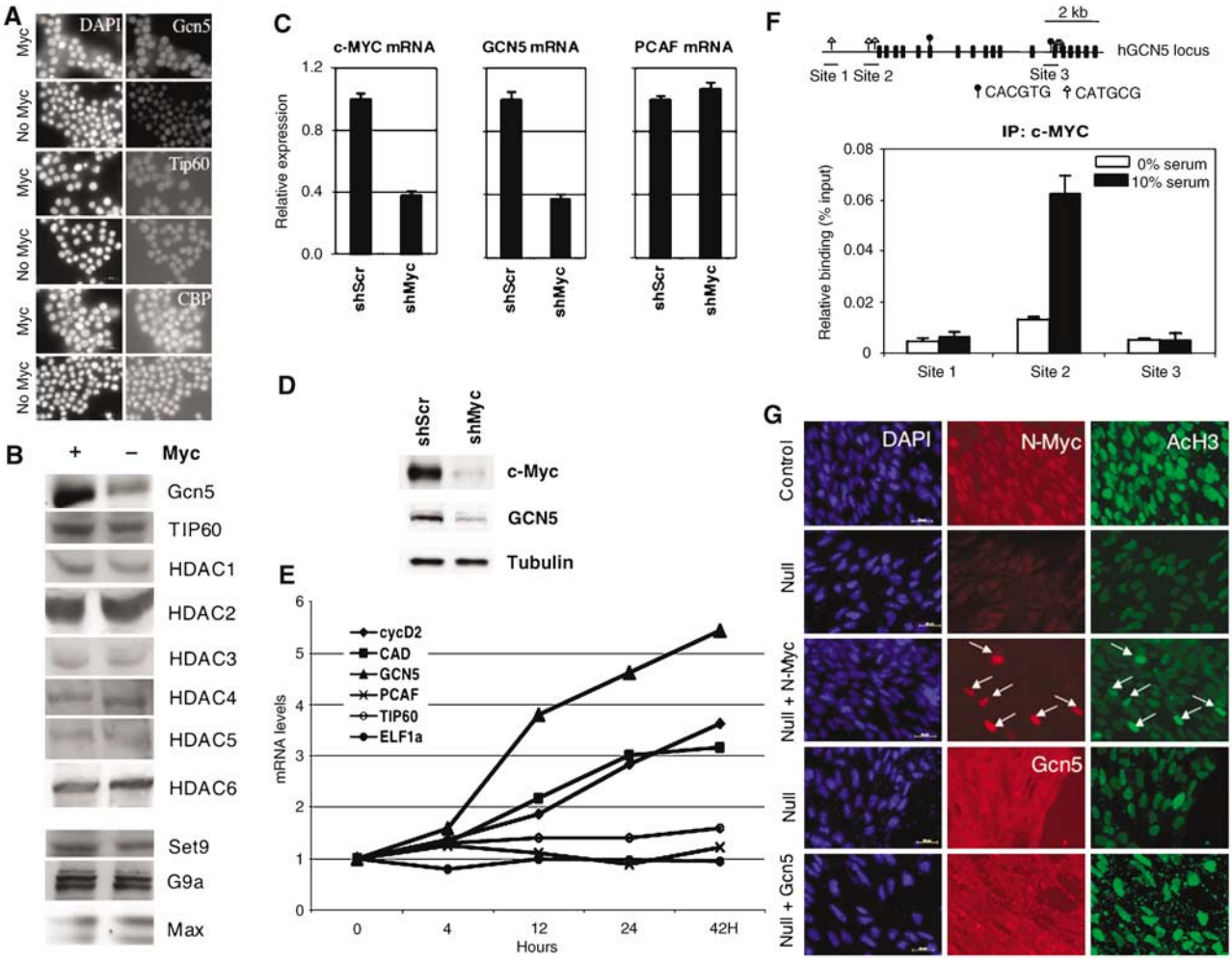

Figure 5 GCN5 is a direct Myc target gene and can reverse histone hypoacetylation in N-*myc* null cells. (**A, B**) Shutting off Myc in the Tet-repressor Myc B cells leads to a reduction in GCN5 levels, but has no effect on the levels of other HATs, HDACs, and HMTs as indicated by IF (monochrome) and immunoblot with antisera against the indicated protein. (**C, D**) shRNA-mediated KD of endogenous Myc results in decreased hGCN5 mRNA levels. Treatment of the human lung cancer cell line H1299 for 48 h with shRNA directed against Myc (shMyc) results in decreased levels of Myc mRNA and protein, whereas a scrambled shRNA (shScr) had no effect. Concomitant with the loss of Myc expression is the loss of hGCN5 at both the protein and mRNA level. (**E**) Myc activates transcription of the hGCN5 gene in primary human cells. The human diploid fibroblast strain IMR90 was stably transduced with a retrovirus directing expression of the Myc-ER protein. Myc-ER-expressing cells were treated with 4-OHT (or EtOH as a negative control) to activate c-Myc for the times indicated. mRNA was harvested and analyzed by quantitative RT–PCR. Actin mRNA levels were determined simultaneously and used to normalize mRNA levels for the other genes. hGCN5 levels are increased by Myc activation even more dramatically than those of the known Myc targets CAD and cyclin D2. Furthermore, mRNA for the other TRRAP-associated HATs, PCAF and TIP60, were not responsive to Myc activation. The non-Myc responsive gene ELF1a was used as a negative control. Values are expressed as fold induction. (**F**) Direct binding of endogenous Myc to the hGCN5 locus *in vivo*. The human GCN5 locus contains two matches to the CACGTG consensus Myc binding site as indicated. In addition, several matches to the non-canonical site bound by Myc in the cytochrome *c* gene (CATGCG) are present. To examine the binding of Myc to these sites, we utilized human diploid fibroblasts that had been either serum deprived or re-fed with 10% FCS for 2 h. Binding of endogenous Myc to three sites within the hGCN5 locus was then assessed. Inducible binding of Myc to site 2, which is adjacent to the transcriptional start site, was evident. (**G**) Overexpression of hGCN5 in N-*myc* null neurospheres reverses histone hypoacetylation as effectively as reintroduction of N-*myc*. Null neurospheres were transfected with N-myc or hGCN5 (red), then IF stained for acetylation of histone H3 (green).

of chromatin-modifying enzymes in Tet-Myc cells or in primary cells with and without Myc were analyzed by IF, immunoblotting, and RT–PCR (Figure 5). Levels of six HDACs (HDACs 1–6), two HATs (TIP60 and CBP), and the two histone methyl transferases (Set9 and G9a) that target H3-K4 and H3-K9 respectively (Peterson and Laniel, 2004) (the methyl marks affected by loss of Myc) were not affected by Myc status (Figure 5A and B). However, the expression of one HAT, GCN5, was strikingly reduced upon loss of Myc at both RNA and protein levels in every system tested. For example, loss of Myc in Tet-off Myc B cells led to strong reductions in GCN5 levels (Figure 5A and B). Similarly, in N-*myc* null neurospheres and CGNPs, levels of GCN5 were strongly reduced (Supplementary Figure S7), whereas levels of other histone-modifying enzymes such as the HATs TIP60, CBP, and p300 were not reduced in Tet-off B cells or in primary N-*myc* null CGNPs. Further, RNAi-mediated knockdown (KD) of c-Myc (Zhang *et al*, 2005) in human cells also caused consistent reductions in GCN5 RNA and protein levels (Figure 5C and D), whereas the levels of another HAT,

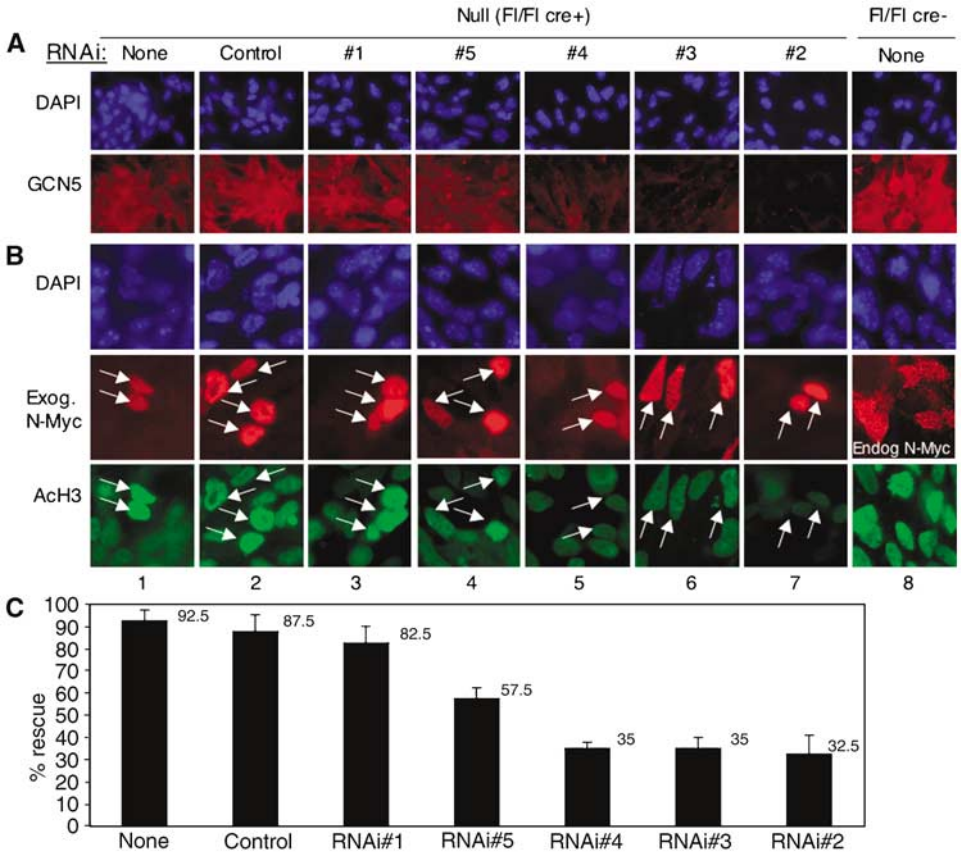

Figure 6 A critical role for GCN5 in Myc's regulation of chromatin. (**A**) RNAi-mediated KD of endogenous GCN5 in N-*myc* null neurospheres. IF analysis with GCN5 antisera (red) indicating variably reduced GCN5 protein levels with five RNAi constructs targeted against GCN5. Column 1, no RNAi treatment; column 2, control RNAi treatment; columns 3–7, treatment with indicated GCN5 RNAi. Columns 1–7 are N-*myc* null neurospheres, whereas column 8 is control neurospheres with no RNAi treatment. (**B**) RNAi KD of endogenous GCN5 blocks the ability of exogenous N-Myc to rescue histone hypoacetylation in N-m*yc* null neurospheres. Representative IF images are shown. Columns 1–7 are cells treated with the same RNAi constructs as in (A) but also followed 48 h later by transfection with exogenous N-Myc (red) and stained for acetylated histone H3 (green) as well as DAPI (blue). Cells expressing exogenous N-Myc are indicated by white arrows. The N-Myc IF panel in column 8 for the Fl/Fl cre− control is from a separate experiment but is included to show representative control levels of endogenous N-Myc protein for comparison. (**C**) Quantitation of the ability of GCN5 RNAi to block rescue. Mean values from four independent groups of 10 N-Myc-transfected cells that were also previously transfected with each type of RNAi are shown with error bars of s.e.m. The differences between the values for the control RNAi and the three strongest RNAi (RNAi #2, #3, and #4) exhibit *P*-values <0.0002, 0.00005, and 0.0009, respectively.

PCAF, were unaffected. Several lines of evidence indicate that GCN5 is a direct Myc target gene. Induction of Myc activity by administration of tamoxifen to primary human fibroblasts stably expressing MycER strongly induced GCN5 expression (Figure 5E), but not expression of other HATs (Tip60, PCAF). Furthermore, chromatin immunoprecipitation (ChIP) assay (Zhang *et al*, 2005) indicates that endogenous Myc directly binds two E-boxes in the GCN5 promoter displaying a 5- to 10-fold increase in binding upon addition of serum (Figure 5F). Serum-inducible Myc occupancy of the GCN5 promoter also correlates with binding of RNA polymerase II as well as histone H3 and H4 acetylation, all signs of gene activation (Supplementary Figure S11). Myc binding to GCN5 is fairly specific as Myc does not detectably bind to HDAC1, HDAC2, Set9, nor PCAF by ChIP assay (Supplementary Figure S11). We did find evidence of Myc binding to TIP60, which contains two E-boxes in its promoter as well; however, because there was no evidence of a link between Myc and TIP60 mRNA or protein expression levels, it remains unclear if Myc regulates TIP60 in this biological setting.

Reduction of endogenous GCN5 levels interferes with Myc-induced hyperacetylation

To more directly assess a potential functional role for GCN5 in Myc's global regulation of chromatin, we employed RNAi to KD endogenous GCN5 utilizing a set of five independent unique GCN5 shRNA constructs (sequence search verified no off-site targets for any of the five constructs), along with a nonspecific control shRNA. The five independent GCN5 RNAi constructs exhibited a range of inhibitory activity that correlated well with reduction in endogenous GCN5 by IF and by Western blot (Figures 6A and Supplementary Figure S8), a target of GCN5's HAT activity, further evidence of the functional specificity of the shRNAs.

If GCN5 is required for Myc's ability to regulate global chromatin, then KD of endogenous GCN5 should block the ability of reintroduced N-Myc to restore the histone acetylation in N-*myc* null neurospheres. Consistent with a critical role for endogenous GCN5 in Myc's global chromatin function, the five GCN5 RNAi constructs interfered with the ability of reintroduced N-Myc to reverse histone hypoacetylation in proportion to their GCN5 KD effectiveness (Figure 6B

and C), whereas the nonspecific RNAi control had no effect. Thus, endogenous GCN5 plays a critical role in Myc's regulation of widespread histone modifications.

Discussion

The notion that Myc is a general chromatin regulator, while to our knowledge unprecedented for an oncoprotein, is nonetheless consistent with several recent observations concerning Myc function. First, a series of independent expression microarray studies have collectively identified an unexpectedly large group of potential genes (representing about 5% of all genes) that are transcriptionally regulated by Myc (Zeller *et al*, 2003). Second, recent experiments directly assessing genomic binding by Myc suggest binding to thousands of sites throughout the genome encompassing approximately 15% of genes as well as intergenic regions (Fernandez *et al*, 2003; Li *et al*, 2003; Orian *et al*, 2003; Cawley *et al*, 2004; Patel *et al*, 2004). Finally, although many Myc target genes are transcribed by RNA polymerase II, Myc has also been shown to directly stimulate both RNA polymerase III and RNA polymerase I transcription (Gomez-Roman *et al*, 2003; Arabi *et al*, 2005; Grandori *et al*, 2005). Thus, the widespread binding of Myc complexes to DNA appears to be linked to pervasive effects on gene expression.

The data presented in this report demonstrate that both loss and gain of Myc function substantially influence widespread histone modifications. Disruption or downregulation of *myc* expression leads to decreased active and increased repressive chromatin marks, an effect that appears to be reversible by overexpression of *myc*. The changes in histone modifications upon loss of *myc* correlate with decreased accessibility of DNA, increases in heterochromatic regions, and decreased nuclear size. We show that these reversible effects are unlikely to be secondary consequences of apoptosis, senescence, differentiation, or loss of proliferative capacity.

How does Myc regulate chromatin on a broad scale? The widespread binding of Myc to genomic DNA and Myc's recruitment of chromatin-modifying complexes to bound loci are likely to contribute to the observed activity. However, widespread binding by Myc is unlikely to fully account for the large-scale effects we observe on chromatin and we believe that additional mechanisms must come into play. Importantly, we have shown that the gene encoding the HAT GCN5 is transcriptionally regulated by Myc and that GCN5 expression is required for introduced Myc to fully reverse the loss of acetylation observed in *myc* null cells. Myc itself recruits GCN5 to its binding sites (McMahon *et al*, 2000); however, we have demonstrated that increased levels of GCN5 alone can strongly augment acetylation in myc null cells (Figure 5G) indicating that GCN5 has widespread effects on chromatin independent of its recruitment by Myc. Indeed, studies in yeast have shown that GCN5 can drive global histone acetylation (Vogelauer *et al*, 2000). We favor the possibility that targeted induction of GCN5 represents a feed-forward mechanism by which Myc augments expression and recruitment of its own HAT while simultaneously permitting additional widespread effects of GCN5 on chromatin. Although additional chromatin-associated factors, including other histone-modifying enzymes as well as those that result in a spreading of chromatin states, may also be recruited by Myc and contribute to its effects on chromatin, GCN5 alone could mediate the effects on acetylation as it has been linked to acetylation of both H3 and H4 in yeast (Kuo *et al*, 1996; Zhang *et al*, 1998). We propose that Myc influences global chromatin structure through both direct (i.e. widespread binding and recruitment of chromatin-modifying activities) and indirect (i.e. induction of GCN5) mechanisms.

Although we also do not know the precise temporal order of the changes we observe, we hypothesize that loss of Myc induces a widespread state of histone hypoacetylation followed by increases in repressive methylation and ultimately nuclear condensation. As recent studies indicate that H3-K4 methylation may direct subsequent histone acetylation, the loss of H3-K4 methylation we observe with disruption of Myc could precede decreased histone acetylation as well (Dou *et al*, 2005; Pray-Grant *et al*, 2005; Wysocka *et al*, 2005)—in this regard, it will be interesting to determine whether Myc recruits histone methyl transferases.

There is considerable interest in possible chromatin-based therapies for cancer (Egger *et al*, 2004) and two recent papers have demonstrated substantial changes in histone modifications associated with specific tumors (Fraga *et al*, 2005; Seligson *et al*, 2005). Because Myc deregulation is linked to the etiology of many different types of tumors, our data suggest a mechanism by which Myc may drive initial changes in chromatin during tumorigenesis. There is currently no evidence that other oncoproteins or transcription factors similarly influence large-scale chromatin structure; however, we would expect that a subset of regulatory proteins with ubiquitous binding sites on DNA might behave like Myc. Thus, our studies provide an example of how other transcription factors and oncoproteins may regulate chromatin on a global scale.

Materials and methods

IHC

Staining of tissue sections was conducted as described (Knoepfler *et al*, 2002). A 1:200 dilution of all antibodies was used.

Immunofluorescence studies

Staining of cultured cells was conducted as described (Knoepfler *et al*, 2002) except that cells were blocked in 5% BSA, 3% NGS, and 0.3% Triton X-100; antibody incubations were conducted in 3% NGS and 0.3% Triton X-100 in PBS. All antibodies were from USB (AcH3: 06-942, AcH4: 06-866, diMeK9: 07-212, triMeK9: 07-422, triMeK4: 07-473, HP1α: 05-689, p300: 05-257, TIP60: 07-389, CBP: 06-294), except N-Myc (Santa Cruz; SC-791 and SC-142), GCN5 (Abcam 18381), and mAb AcH3 (Abcam 12179). A 1:500 dilution was used in each case. Mean fluorescence intensity was determined using Photoshop by subtracting the value of background fluorescence (areas with no nuclei) from fluorescence from nuclei.

Electron microscopy

Cultured CGNPs were embedded in Epon. Processing and imaging was conducted as described (Morrish *et al*, 2003).

Preparation, culture, and transfection/infection of cells

CGNPs were isolated and cultured as described (Kenney *et al*, 2003). Neurospheres were isolated and cultured as described (Knoepfler *et al*, 2002). Virus was produced as described (Knoepfler *et al*, 2002) except that the helper plasmid was VSV-G and the virus was concentrated by centrifugation at 30 000 *g* for 30 min. Neurospheres were transfected with Fugene-6. In the rescue experiment in neurospheres, N-MycER and N-MycERΔMBII were used with tamoxifen treatment or WT N-Myc was used. TSA treatment of cells was at 100 ng/ml for 20 h. In the experiments looking at

induction of GCN5 by Myc, c-MycER was used as described (Zhang *et al*, 2005).

Knockout and transgenic mice

The production and use of the N-*myc* and c-*myc* conditional knockout mice have been described (de Alboran *et al*, 2001; Knoepfler *et al*, 2002). Although derived from the same ES cell line, the N-$myc^{flox/flox}$ mice used in the current study do not retain a neo cassette. The same nestin-cre Tg mice were used as before (Knoepfler *et al*, 2002). As the nestin-cre Tg activity is moderately leaky in gametes, some mice used in these studies are flox/flox and some are flox/null, but there is no consistent phenotypic difference between flox/flox and flox/null mice. The N-*myc* Tg mice were produced by pronuclear injection of a Tg vector designed to express N-MycER-IRES-GFP. Nine founder strains were established; data are from Tg embryos from two founders.

Immunoblotting/ChIP

Equal amounts of total protein from acid-extracted histones, prepared as described (McKittrick *et al*, 2004), were used. Blots were probed with the indicated antibodies and analyzed using the Odyssey system as directed by the manufacturer (LI-COR). Quantitative data for relative histone acetylation are the mean from two separate experiments on unique extracts, whereas data for methylation are from one experiment. Antibody dilutions were 1:1000 for all antibodies with the exception of 1:5000 for triMeK9 and triMeK4. ChIP was conducted as follows. NHDF (2091) cells were plated on 15-cm dishes, incubated for 24 h, and then deprived of growth factors for a subsequent 24 h by incubation in 0.1% serum-containing medium. After 0 or 2 h of serum stimulation (10%), cells were fixed in 1% formaldehyde. Chromatin was sheared to an average size of 500–1000 bp by sonication (6–8 times with 10-s pulses, 30% output on a Branson Model 250). Lysates corresponding to 5–10 million cells were rotated at 4°C overnight with 2 μg of polyclonal antibodies specific for c-MYC (sc-764, Santa Cruz Biotechnology). Precipitated DNA fragments were quantified by using qPCR. Experiments were performed in triplicate, and normalized by input DNA.

RNAi

Five independent shRNA expression plasmids targeted against mGCN5 were used according to the manufacturer's instructions (Sigma). RNAi constructs #1–5 are shRNAs with a 21 bp stem (6 bp loop) with homology against mGCN5 sequences beginning at the following base-pairs of the coding region: (1) 280, (2) 841, (3) 941, (4) 1770, and (5) 1996. For specific sequences of each construct and other details, see http://www.sigmaaldrich.com/catalog/search/ProductDetail/SIGMA/SHDNA-NM_020004. Verification of the absence of off-site targets was conducted by blastn search of the non-redundant database (Altschul *et al*, 1990). The control RNAi was an shRNA against the empty vector pBS. The plasmids were transiently transfected into N-*myc* null neurospheres using Fugene-6. After 24 h, cells were transfected with either empty vector or N-Myc, and then 48 h after the second transfection, cells were harvested. Effectiveness of KD of GCN5 was analyzed by IF staining for GCN5, whereas blockage of rescue was gauged by double IF staining for AcH3 and N-Myc. Four randomly selected sets of 10 clearly N-Myc-transfected cells (strongly N-Myc positive N-*myc* null cells) of each type were analyzed by AcH3 levels and scored as rescued if they exhibited AcH3 levels clearly above the surrounding untransfected cells. RNAi against c-Myc was conducted as described (Zhang *et al*, 2005).

MNase accessibility assay

Assays were conducted as described (Zaret, 1999). Briefly, living cells were permeabilized on ice with lysolecithin and then treated with various concentrations of MNase for 5 min. DNA was purified by phenol/chloroform extraction and 10 μg was loaded on 1.2% agarose gels. Only 2.5 μg of DNA from the 0 MNase samples was loaded to avoid smearing of the highly viscous undigested DNA; however, at 10 or even 20 μg of DNA, there was no evidence of endogenous nuclease activity in either sample despite smearing.

HPLC and MS

Isolated histone mixtures were adjusted to 0.1% trifluoroacetic acid and 30% acetonitrile and separated by HPLC as described (McKittrick *et al*, 2004). Analysis of histone H4 used an established derivitization-based MS technique that combines isotopic labeling with tandem mass spectrometry to determine the percentage of acetylation at each lysine within the amino-terminal peptide 4-GKGGKGLGKGGAKR-17 of H4 (Smith *et al*, 2003). Mass spectrometry analyses were performed on an LTQ-FT (ThermoElectron) hybrid mass spectrometer configured for microcapillary LC-MS (Gatlin *et al*, 1998). High-resolution MS was conducted in the FTICR portion of the instrument to determine the proportion of unacetylation, mono-, di-, tri-, and tetra-acetylation on the above H4 peptide. Measurements to determine the distribution of acetylation on the lysines in the H4 peptide were conducted by MS/MS in the ion trap portion of the instrument.

Supplementary data

Supplementary data are available at *The EMBO Journal* Online.

Acknowledgements

We thank Ignacio Moreno de Alboran for the c-*myc* flox/flox mice, Tina Xu for excellent technical assistance, Anna Kenney and David Rowitch for teaching us CGNP culture and for reagents, Amir Orian for sharing unpublished data, John Sedivy and Yuzuru Shiio for the c-*myc* null rat fibroblasts, and Bobbie Schneider and the FHCRC EM staff for excellent technical help. We are indebted to Samir Hanash for access to the LTQ-FT and to Hong Wang and Doug Phanstiel for collection of the mass spectrometry data. We also thank Steve Henikoff, Mark Groudine, Susan Mendrysa, Julie Secombe, and Amir Orian for critical reading of the manuscript. We also thank Santa Cruz Biotechnology for help with antibodies. The authors have no competing interests. This work was supported by NIH/NCI grant CA20525 to RNE and KOICA114400-01 to PSK. RNE is an American Cancer Society Professor.

References

Altschul SF, Gish W, Miller W, Myers EW, Lipman DJ (1990) Basic local alignment search tool. *J Mol Biol* **215:** 403–410

Arabi A, Wu S, Ridderstrale K, Bierhoff H, Shiue C, Fatyol K, Fahlen S, Hydbring P, Soderberg O, Grummt I, Larsson LG, Wright AP (2005) c-Myc associates with ribosomal DNA and activates RNA polymerase I transcription. *Nat Cell Biol* **7:** 303–310

Aruga J, Yokota N, Hashimoto M, Furuichi T, Fukuda M, Mikoshiba K (1994) A novel zinc finger protein, zic, is involved in neurogenesis, especially in the cell lineage of cerebellar granule cells. *J Neurochem* **63:** 1880–1890

Ayer DE (1999) Histone deacetylases: transcriptional repression with siners and nurds. *Trends Cell Biol* **9:** 193–198

Bannister AJ, Zegerman P, Partridge JF, Miska EA, Thomas JO, Allshire RC, Kouzarides T (2001) Selective recognition of methylated lysine 9 on histone H3 by the HP1 chromo domain. *Nature* **410:** 120

Baxter J, Sauer S, Peters A, John R, Williams R, Caparros ML, Arney K, Otte A, Jenuwein T, Merkenschlager M, Fisher AG (2004) Histone hypomethylation is an indicator of epigenetic plasticity in quiescent lymphocytes. *EMBO J* **23:** 4462–4472

Berger SL, Felsenfeld G (2001) Chromatin goes global. *Mol Cell* **8:** 263

Bickmore WA, Craig JM (1997) *Chromosome Bands: Patterns in the Genome*. Heidelberg: Springer

Braunstein M, Sobel RE, Allis CD, Turner BM, Broach JR (1996) Efficient transcriptional silencing in *Saccharomyces cerevisiae* requires a heterochromatin histone acetylation pattern. *Mol Cell Biol* **16:** 4349

Busch H (1974) *The Cell Nucleus*. New York: Academic Press

Cawley S, Bekiranov S, Ng HH, Kapranov P, Gingeras TR (2004) Unbiased mapping of transcription factor binding sites along human chromosomes 21 and 22 points to widespread regulation of noncoding RNAs. *Cell* **116:** 499–509

Cheng S-WG, Davies KP, Yung E, Beltran RJ, Yu J, Kalpana GV (1999) c-MYC interacts with INI1/hSNF5 and requires the SWI/SNF complex for activation function. *Nat Genet* **22:** 102–105

Cohen M, Lee KK, Wilson KL, Gruenbaum Y (2001) Transcriptional repression, apoptosis, human disease and the functional evolution of the nuclear lamina. *Trends Biochem Sci* **26:** 41–47

Davis AC, Wims M, Spotts GD, Hann SR, Bradley A (1993) A null c-myc mutation causes lethality before 10.5 days of gestation in homozygous and reduced fertility in heterozygous female mice. *Genes Dev* **7:** 671–682

de Alboran IM, O'Hagan RC, Gartner F, Malynn B, Davidson L, Rickert R, Rajewsky K, DePinho RA, Alt FW (2001) Analysis of C-MYC function in normal cells via conditional gene-targeted mutation. *Immunity* **14:** 45–55

Dou Y, Milne TA, Tackett AJ, Smith ER, Fukuda A, Wysocka J, Allis CD, Chait BT, Hess JL, Roeder RG (2005) Physical association and coordinate function of the H3 K4 methyltransferase MLL1 and the H4 K16 acetyltransferase MOF. *Cell* **121:** 873–885

Egger G, Liang G, Aparicio A, Jones PA (2004) Epigenetics in human disease and prospects for epigenetic therapy. *Nature* **429:** 457–463

Eisenman RN (2001) Deconstructing myc. *Genes Dev* **15:** 2023–2030

Fernandez PC, Frank SR, Wang L, Schroeder M, Liu S, Greene J, Cocito A, Amati B (2003) Genomic targets of the human c-Myc protein. *Genes Dev* **17:** 1115–1129

Fraga MF, Ballestar E, Villar-Garea A, Boix-Chornet M, Espada J, Schotta G, Bonaldi T, Haydon C, Ropero S, Petrie K, Iyer NG, Perez-Rosado A, Calvo E, Lopez JA, Cano A, Calasanz MJ, Colomer D, Piris MA, Ahn N, Imhof A, Caldas C, Jenuwein T, Esteller M (2005) Loss of acetylation at Lys16 and trimethylation at Lys20 of histone H4 is a common hallmark of human cancer. *Nat Genet* **37:** 391–400

Frank SR, Parisi T, Taubert S, Fernandez P, Fuchs M, Chan HM, Livingston DM, Amati B (2003) MYC recruits the TIP60 histone acetyltransferase complex to chromatin. *EMBO Rep* **4:** 575–580

Frank SR, Schroeder M, Fernandez P, Taubert S, Amati B (2001) Binding of c-Myc to chromatin mediates mitogen-induced acetylation of histone H4 and gene activation. *Genes Dev* **15:** 2069

Gatlin CL, Kleemann GR, Hays LG, Link AJ, Yates III JR (1998) Protein identification at the low femtomole level from silver-stained gels using a new fritless electrospray interface for liquid chromatography-microspray and nanospray mass spectrometry. *Anal Biochem* **263:** 93–101

Gerdes J, Li L, Schlueter C, Duchrow M, Wohlenberg C, Gerlach C, Stahmer I, Kloth S, Brandt E, Flad HD (1991) Immunobiochemical and molecular biologic characterization of the cell proliferation-associated nuclear antigen that is defined by monoclonal antibody Ki-67. *Am J Pathol* **138:** 867–873

Gomez-Roman N, Grandori C, Eisenman RN, White RJ (2003) Direct activation of RNA polymerase III transcription by c-Myc. *Nature* **421:** 290–294

Grandori C, Gomez-Roman N, Felton-Edkins ZA, Ngouenet C, Galloway DA, Eisenman RN, White RJ (2005) c-Myc binds to human ribosomal DNA and stimulates transcription of rRNA genes by RNA polymerase I. *Nat Cell Biol* **7:** 311–318

Grandori C, Wu KJ, Fernandez P, Ngouenet C, Grim J, Clurman BE, Moser MJ, Oshima J, Russell DW, Swisshelm K, Frank S, Amati B, Dalla-Favera R, Monnat Jr RJ (2003) Werner syndrome protein limits MYC-induced cellular senescence. *Genes Dev* **17:** 1569–1574

Iritani BM, Delrow J, Grandori C, Gomez I, Klacking M, Carlos LS, Eisenman RN (2002) Modulation of T lymphocyte development, growth, and cell size by the Myc-antagonist Mad1 transcriptional repressor. *EMBO J* **21:** 4820–4830

Jeppesen P, Turner BM (1993) The inactive X chromosome in female mammals is distinguished by a lack of histone H4 acetylation, a cytogenetic marker for gene expression. *Cell* **74:** 281

Kenney AM, Cole MD, Rowitch DH (2003) Nmyc upregulation by sonic hedgehog signaling promotes proliferation in developing cerebellar granule neuron precursors. *Development* **130:** 15–28

Knoepfler PS, Cheng PF, Eisenman RN (2002) N-*myc* is essential during neurogenesis for the rapid expansion of progenitor cell populations and the inhibition of neuronal differentiation. *Genes Dev* **16:** 2699–2712

Knoepfler PS, Eisenman RN (1999) Sin meets NuRD and other tails of repression. *Cell* **99:** 447–450

Kuo MH, Brownell JE, Sobel RE, Ranalli TA, Cook RG, Edmondson DG, Roth SY, Allis CD (1996) Transcription-linked acetylation by Gcn5p of histones H3 and H4 at specific lysines. *Nature* **383:** 269–272

Kurdistani SK, Tavazoie S, Grunstein M (2004) Mapping global histone acetylation patterns to gene expression. *Cell* **117:** 721

Lachner M, O'Carroll D, Rea S, Mechtler K, Jenuwein T (2001) Methylation of histone H3 lysine 9 creates a binding site for HP1 proteins. *Nature* **410:** 116

Li Z, Van Calcar S, Qu C, Cavenee WK, Zhang MQ, Ren B (2003) A global transcriptional regulatory role for c-Myc in Burkitt's lymphoma cells. *Proc Natl Acad Sci USA* **100:** 8164–8169

Lutz W, Leon J, Eilers M (2002) Contributions of Myc to tumorigenesis. *Biochim Biophys Acta* **1602:** 61–71

Mateyak MK, Obaya AJ, Adachi S, Sedivy JM (1997) Phenotypes of c-myc-deficient rat fibroblasts isolated by targeted homologous recombination. *Cell Growth Differ* **8:** 1039–1048

McKittrick E, Gafken PR, Ahmad K, Henikoff S (2004) Histone H3.3 is enriched in covalent modifications associated with active chromatin. *Proc Natl Acad Sci USA* **101:** 1525–1530

McMahon SB, Van Buskirk HA, Dugan KA, Copeland TD, Cole MD (1998) The novel ATM-related protein TRRAP is an essential cofactor for the c-Myc and E2F oncoproteins. *Cell* **94:** 363–374

McMahon SB, Wood MA, Cole MD (2000) The essential cofactor TRRAP recruits the histone acetyltransferase hGCN5 to c-Myc. *Mol Cell Biol* **20:** 556–562

Morrish F, Giedt C, Hockenbery D (2003) c-MYC apoptotic function is mediated by NRF-1 target genes. *Genes Dev* **17:** 240–255

Orian A, van Steensel B, Delrow J, Bussemaker HJ, Li L, Sawado T, Williams E, Loo LM, Cowley SM, Yost C, Pierce S, Edgar BA, Parkhurst SM, Eisenman RN (2003) Genomic binding by the *Drosophila* Myc, Max, Mad. Mnt transcription factor network. *Genes Dev* **17:** 1101–1114

Patel JH, Loboda AP, Showe MK, Showe LC, McMahon SB (2004) Analysis of genomic targets reveals complex functions of MYC. *Nat Rev Cancer* **4:** 562

Peterson CL, Laniel MA (2004) Histones and histone modifications. *Curr Biol* **14:** R546–R551

Pray-Grant MG, Daniel JA, Schieltz D, Yates 3rd JR, Grant PA (2005) Chd1 chromodomain links histone H3 methylation with SAGA- and SLIK-dependent acetylation. *Nature* **433:** 434–438

Rea S, Eisenhaber F, O'Carroll D, Strahl BD, Sun ZW, Schmid M, Opravil S, Mechtler K, Ponting CP, Allis CD, Jenuwein T (2000) Regulation of chromatin structure by site-specific histone h3 methyltransferases. *Nature* **406:** 593–599

Schubeler D, MacAlpine DM, Scalzo D, Wirbelauer C, Kooperberg C, van Leeuwen F, Gottschling DE, O'Neill LP, Turner BM, Delrow J, Bell SP, Groudine M (2004) The histone modification pattern of active genes revealed through genome-wide chromatin analysis of a higher eukaryote. *Genes Dev* **18:** 1263–1271

Schuhmacher M, Staege MS, Pajic A, Polack A, Weidle UH, Bornkamm GW, Eick D, Kohlhuber F (1999) Control of cell growth by c-Myc in the absence of cell division. *Curr Biol* **9:** 1255–1258

Seligson DB, Horvath S, Shi T, Yu H, Tze S, Grunstein M, Kurdistani SK (2005) Global histone modification patterns predict risk of prostate cancer recurrence. *Nature* **435:** 1262–1266

Shen-Li H, O'Hagan RC, Hou HJ, Horner JW, Lee HW, DePinho RA (2000) Essential role for Max in early embryonic growth and development. *Genes Dev* **14:** 17–22

Shiio Y, Donohoe S, Yi EC, Goodlett DR, Aebersold R, Eisenman RN (2002) Quantitative proteomic analysis of Myc oncoprotein function. *EMBO J* **21:** 5088–5096

Shogren-Knaak M, Ishii H, Sun JM, Pazin MJ, Davie JR, Peterson CL (2006) Histone H4-K16 acetylation controls chromatin structure and protein interactions. *Science* **311:** 844–847

Smith CM, Gafken PR, Zhang Z, Gottschling DE, Smith JB, Smith DL (2003) Mass spectrometric quantification of acetylation at specific lysines within the amino-terminal tail of histone H4. *Anal Biochem* **316:** 23–33

Stanton BR, Perkins AS, Tessarollo L, Sassoon DA, Parada LF (1992) Loss of N-*myc* function results in embryonic lethality and failure of the epithelial component of the embryo to develop. *Gene Dev* **6:** 2235–2247

Strahl BD, Allis CD (2000) The language of covalent histone modifications. *Nature* **403:** 41–45

Turner BM, Birley AJ, Lavender J (1992) Histone H4 isoforms acetylated at specific lysine residues define individual chromosomes and chromatin domains in *Drosophila* polytene nuclei. *Cell* **69:** 375

Vervoorts J, Luscher-Firzlaff JM, Rottmann S, Lilischkis R, Walsemann G, Dohmann K, Austen M, Luscher B (2003) Stimulation of c-MYC transcriptional activity and acetylation by recruitment of the cofactor CBP. *EMBO Rep* **4:** 1–7

Vogelauer MWJ, Suka N, Grunstein M (2000) Global histone acetylation and deacetylation in yeast. *Nature* **408:** 495

Wakamatsu Y, Watanabe Y, Shimono A, Kondoh H (1993) Transition of localization of the N-Myc protein from nucleus to cytoplasm in differentiating neurons. *Neuron* **10:** 1–9

Weintraub H, Groudine M (1976) Chromosomal subunits in active genes have an altered conformation. *Science* **193:** 848–856

Wysocka J, Swigut T, Milne TA, Dou Y, Zhang X, Burlingame AL, Roeder RG, Brivanlou AH, Allis CD (2005) WDR5 associates with histone H3 methylated at K4 and is essential for H3 K4 methylation and vertebrate development. *Cell* **121:** 859–872

Zaret K (1999) Micrococcal nuclease analysis of chromatin structure. In *Current Protocols in Molecular biology*, Ausubel FM, Kingston RBRE, Moore DD, Seidman JG, Smith JA, Struhl K (eds) Vol. 3, pp 21.1.1–21.1.17. New York: Wiley

Zeller KI, Jegga AG, Aronow BJ, O'Donnell KA, Dang CV (2003) An integrated database of genes responsive to the Myc oncogenic transcription factor: identification of direct genomic targets. *Genome Biol* **4:** R69

Zhang W, Bone JR, Edmondson DG, Turner BM, Roth SY (1998) Essential and redundant functions of histone acetylation revealed by mutation of target lysines and loss of the Gcn5p acetyltransferase. *EMBO J* **17:** 3155–3167

Zhang XY, Desalle LM, Patel JH, Capobianco AJ, Yu D, Thomas-Tikhonenko A, McMahon SB (2005) Metastasis-associated protein 1 (MTA1) is an essential downstream effector of the c-MYC oncoprotein. *Proc Natl Acad Sci USA* **102:** 13968–13973

